FABAD J. Pharm. Sci., 51, 3, 1373-1390, 2026
Doi: 10.55262/fabadeczacilik.1993906
RESEARCH ARTICLE

Development and Characterization of an Amaranth Oil Nanoemulgel Incorporating Nisin and Hydrolyzed Wheat Protein for Topical Delivery in Atopic Dermatitis

Ebru ALTUNTAŞ[*°], Ceren KOCA[**], Müzeyyen AYDIN[***]

Development and Characterization of an Amaranth Oil Nanoemulgel Incorporating Nisin and Hydrolyzed Wheat Protein for Topical Delivery in Atopic Dermatitis

SUMMARY

Atopic dermatitis is a chronic inflammatory skin disease associated with impaired skin barrier function and increased susceptibility to bacterial colonization, particularly by Staphylococcus aureus. In this study, an amaranth oil nanoemulgel containing nisin and hydrolyzed wheat protein was developed and characterized as a potential topical delivery system for atopic dermatitis. Initially, sixteen nanoemulsion formulations prepared using different surfactant systems were evaluated in terms of droplet size, polydispersity index (PDI), zeta potential, visual appearance, and short-term physical stress testing. Two nanoemulsions selected from the screening results were subsequently combined with xanthan gum hydrogel bases of different polymer concentrations to obtain nanoemulgels. The formulations were characterized for their physicochemical properties, short-term physical stress testing, pH, electrical conductivity, rheological behavior, and antibacterial activity against Staphylococcus aureus ATCC 29213 and Staphylococcus epidermidis ATCC 12228. Based on the combined assessment of physicochemical findings, homogeneous appearance, and gel consistency, the Cremophor® RH40-based nanoemulgel prepared with the hydrogel base containing 1.5% xanthan gum was selected for further evaluation. The selected formulation exhibited pseudoplastic flow behavior. Both nisin-loaded nanoemulgels demonstrated antibacterial activity against the tested bacterial strains, whereas no antibacterial activity was observed for the corresponding placebo formulations. These findings support further evaluation of the nanoemulgel as a potential topical formulation containing nisin; however, nisin release and skin delivery were not measured and require investigation in future studies.

Keywords: *Atopic dermatitis, nanoemulgel, nisin, amaranth oil, antimicrobial activity, topical drug delivery*

Atopik Dermatitin Topikal Tedavisi İçin Nisin ve Hidrolize Buğday Proteini İçeren Amarant Yağı Nanoemüljelinin Geliştirilmesi ve Karakterizasyonu

ÖZ

Atopik dermatit, deri bariyerinin bozulması ve özellikle Staphylococcus aureus kolonizasyonundaki artış ile karakterize kronik inflamatuvar bir deri hastalığıdır. Bu çalışmada, atopik dermatitin topikal tedavisine yönelik hidrolize buğday proteini ve nisin içeren amarant yağı nanoemüljeli geliştirilmiş ve karakterize edilmiştir. İlk aşamada farklı yüzey aktif madde sistemleri kullanılarak hazırlanan on altı nanoemülsiyon; damlacık boyutu, polidispersite indeksi (PDI), zeta potansiyeli, görsel özellikleri ve kısa süreli fiziksel stres testleri açısından değerlendirilmiştir. Tarama sonuçlarına göre seçilen iki nanoemülsiyon, farklı ksantan zamkı konsantrasyonlarına sahip hidrojel bazlarıyla birleştirilerek nanoemüljeller hazırlanmıştır. Formülasyonların fizikokimyasal özellikleri, kısa süreli fiziksel stres testleri, pH, elektriksel iletkenliği, reolojik davranışı ile Staphylococcus aureus ATCC 29213 ve Staphylococcus epidermidis ATCC 12228'ye karşı antibakteriyel aktiviteleri incelenmiştir. Formülasyonların fizikokimyasal bulguları, homojen görünümü ve jel kıvamı birlikte değerlendirilerek, %1,5 ksantan zamkı içeren hidrojel bazından hazırlanan Cremophor® RH40 esaslı nanoemüljel ileri değerlendirme için seçilmiştir. Seçilen formülasyon psödoplastik akış davranışı göstermiştir. Nisin içeren nanoemüljeller her iki bakteri suşuna karşı antibakteriyel aktivite gösterirken, plasebo formülasyonlarda herhangi bir antibakteriyel etki gözlenmemiştir. Sonuçlar, geliştirilen nanoemüljelin nisin içeren potansiyel bir topikal formülasyon olarak ileri değerlendirmeye değer olduğunu göstermektedir. Bununla birlikte, nisinin formülasyondan salımı ve deriye iletimi bu çalışmada ölçülmemiştir; bu özelliklerin nicel salım testleri ve ileri biyolojik çalışmalarla değerlendirilmesi gerekmektedir.

Anahtar Kelimeler: *Atopik dermatit, nanoemüljel, nisin, amarant yağı, antimikrobiyal aktivite, topikal ilaç dağıtımı*

Recieved: 13.07.2026
Revised: 01.10.2026
Accepted: 06.10.2026

* ORCID: 0000-0003-2902-5554, İstanbul University, Faculty of Pharmacy, Department of Pharmaceutical Technology, Istanbul, Türkiye
** ORCID: 0000-0002-9972-0176, İstanbul University, Faculty of Pharmacy, Department of Pharmaceutical Technology, Istanbul, Türkiye; İstanbul University, Graduate School of Health Sciences, Istanbul, Türkiye
*** ORCID: 0000-0002-8082-9470, Department of Pharmaceutical Microbiology, Faculty of Pharmacy, İstanbul University, Istanbul, Türkiye; İstanbul University, Graduate School of Health Sciences, Istanbul, Türkiye

° Corresponding Author; Ebru Altuntaş
E-mail: ebru.altuntas@istanbul.edu.tr

INTRODUCTION

Atopic dermatitis (AD) is one of the most common chronic inflammatory skin disorders, affecting approximately 15–25% of children and 3–10% of adults worldwide, with an increasing prevalence reported over recent decades (Eichenfield et al., 2022). It is characterized by recurrent eczematous lesions, intense pruritus, xerosis, and relapsing flares, and arises from a complex interaction among genetic susceptibility, epidermal barrier dysfunction, immune dysregulation, environmental triggers, and microbial imbalance (Kim, Kim, Ahn, & Leung, 2019). Beyond its cutaneous manifestations, AD markedly impairs quality of life and imposes a considerable socioeconomic burden because of its chronic relapsing nature (Kwatra, Gruben, Fung, & DiBonaventura, 2021). Epidermal barrier impairment, characterized by reduced filaggrin expression, altered lipid composition, increased transepidermal water loss, and cytokine-mediated suppression of structural proteins, facilitates the penetration of allergens and microbial pathogens, thereby perpetuating chronic inflammation (Bhattacharya, Sato, Kelly, Ganguli-Indra, & Indra, 2019; Goleva, Berdyshev, & Leung, 2019; Hatano & Elias, 2023). This impaired barrier also favors cutaneous microbial dysbiosis, most notably the overgrowth of *Staphylococcus aureus (S. aureus)*, which is frequently observed in AD lesions and correlates with disease severity (Chen, Knight, & Gallo, 2023).

S. aureus is considered the predominant bacterial pathogen associated with AD and contributes directly to disease exacerbation. *S. aureus* aggravates AD through biofilm formation and secretion of virulence factors that disrupt epidermal integrity and amplify Th2-driven inflammation (Byrd et al., 2017; Gonzalez et al., 2021; Kim et al., 2019; Totté et al., 2016).

Current topical management of atopic dermatitis relies on corticosteroids, calcineurin inhibitors, moisturizers, barrier-repair products, and topical antibiotics (Wollenberg et al., 2020). However, their long-term use is limited by frequent relapse, poor adherence, corticosteroid-related adverse effects, and increasing antimicrobial resistance (George et al., 2019; Tier et al., 2021). Therefore, the development of topical formulations with both antimicrobial and skin-supportive properties remains an important therapeutic strategy.

Nisin, a naturally occurring lantibiotic produced by *Lactococcus lactis*, has attracted considerable interest as an alternative antimicrobial agent because of its potent activity against Gram-positive bacteria, favorable safety profile, and low propensity for resistance development (Dijksteel, Ulrich, Middelkoop, & Boekema, 2021; Draper, Cotter, Hill, & Ross, 2015). Its antibacterial activity is primarily mediated through binding to lipid II, leading to inhibition of cell wall synthesis and membrane pore formation (Wiedemann et al., 2001). In addition to its antibacterial and antibiofilm activity against *S. aureus*, nisin has been investigated in several topical delivery approaches. Valenta et al. (1996) evaluated the antistaphylococcal activity of nisin in different topical formulations as a potential approach for *S. aureus*-associated atopic dermatitis. More recently, nisin has been incorporated into a Carbopol-based gel for the treatment of infected burn wounds (Preet, Kaur, & Raza, 2021) and into lipid nanoparticles embedded in gellan gum/alginate-based wound dressings for controlled antimicrobial delivery (Reczyńska-Kolman, Hartman, Kwiecień, Brzychczy-Włoch, & Pamuła, 2021). These studies demonstrate the feasibility of incorporating nisin into semisolid and nanostructured topical delivery platforms. However, its topical application is limited by pH-dependent instability, enzymatic degradation, and short skin residence time, highlighting the need for suitable delivery systems to improve its local stability and antimicrobial efficacy (de Alcantara Sica de Toledo, Rosseto, Buccini, & Franco, 2025; Tavares, Ribeiro, Silva, Antunes, & Felgueiras, 2024).

In this context, amaranth oil and hydrolyzed wheat protein were selected as formulation components based on their reported emollient and skin-con-

ditioning properties, respectively. Amaranth oil is rich in bioactive lipids, including squalene, linoleic acid, tocopherols, and phytosterols, which have been associated with antioxidant, emollient, and skin barrier-supporting properties (Martirosyan, Hutcheson, Sajitharan, Williams, & Mohan, 2021; Nasirpour-Tabrizi, Azadmard-Damirchi, Hesari, & Piravi-Vanak, 2020). Hydrolyzed wheat protein is used as a skin-conditioning and film-forming ingredient in cosmetic formulations (Burnett et al., 2018). Its potential contribution to skin hydration or barrier function was not assessed in the present study.

Nanoemulsions are promising topical delivery systems because they improve the solubility, stability, and skin deposition of active compounds while promoting close contact with the skin surface (Lal, Kumar, Saeedan, & Ansari, 2023; Nastiti et al., 2017). Incorporation of nanoemulsions into gel matrices produces nanoemulgels, which combine the dispersed oil droplets of nanoemulsions with the semisolid consistency and rheological properties imparted by the hydrogel matrix (Ijaz et al., 2025; Jacob & Nair, 2026; Sghier, Mur, Veiga, Paiva-Santos, & Pires, 2024). These characteristics make nanoemulgels attractive carriers for topical drug delivery.

Although nisin has previously been investigated in different topical delivery systems, including formulations intended for *S. aureus*-associated atopic dermatitis, studies combining nisin with amaranth oil and hydrolyzed wheat protein in a nanoemulgel platform remain limited. Therefore, this exploratory study aimed to develop an amaranth oil nanoemulgel containing hydrolyzed wheat protein and nisin added to the xanthan gum gel base after preparation of the nisin-free nanoemulsion, and to evaluate its physicochemical properties, performance under short-term physical stress conditions, rheological behavior, and preliminary antibacterial activity against *S. aureus* and *S. epidermidis*. Quantitative nisin release was not assessed in this formulation screening study.

MATERIALS AND METHODS

Materials

Nisin (≥95% purity), Quillaja saponin, Poloxamer 188, DL-α-tocopheryl acetate, Cremophor® RH40, and PEG 400 were purchased from Sigma-Aldrich (St. Louis, MO, USA). Amaranth oil was supplied by Pharmix Bitkisel İlaç ve Kozmetik Sanayi (İstanbul, Türkiye). Caprylic/capric triglyceride (Labrafac™ WL 1349), Labrasol®, and Transcutol® HP were kindly supplied by Gattefossé (Saint-Priest, France). Sensiva® PA 30 was provided by Ashland (Wilmington, DE, USA). Xanthan gum was obtained from Vanderbilt Minerals, LLC (Norwalk, CT, USA). Hydrolyzed wheat protein (Kemigran® 40) was supplied by Kalichem S.r.l. (Bologna, Italy). Ultrapure water was used for the preparation of all formulations. All chemicals and reagents used in this study were of analytical grade and were used without further purification.

Preparation of nanoemulsions

Nanoemulsions were prepared using the probe ultrasonication method (Kumar, Bishnoi, Shukla, & Jain, 2019; Malik, Nawaz, & Noor, 2024). The oil phase consisted of DL-α-tocopheryl acetate (0.2%, w/w), amaranth oil (2%, w/w), caprylic/capric triglyceride (3.3%, w/w), Sensiva® PA 30 (2%, w/w), Labrasol® (2.5%, w/w), and Transcutol® HP (2.5%, w/w). The components were mixed under magnetic stirring until a homogeneous oil phase was obtained. Given its peptide structure and the potential risk of degradation under demanding processing conditions, nisin was incorporated into the aqueous xanthan gum gel base after preparation of the nisin-free nanoemulsion. This precautionary sequence avoided exposing nisin to the probe ultrasonication and heating steps used during nanoemulsion preparation.

The aqueous phase was prepared according to the formulation design using different surfactant systems (Poloxamer 188, Cremophor® RH40, Quillaja saponin, or their combinations). Kemigran® 40 was included at 1% (w/w) in all nanoemulsions, while PEG

400 was incorporated into selected formulations. Following the 1:1 (w/w) mixing of nanoemulsion and hydrogel, the final concentration of Kemigran® 40, as supplied, was 0.5% (w/w) in each nanoemulgel. All components were dissolved in ultrapure water under magnetic stirring, and formulations containing Cremophor® RH40 or Quillaja saponin were heated to approximately 40 °C to facilitate dissolution before cooling to room temperature.

The aqueous phase was gradually added to the oil phase under magnetic stirring to obtain a coarse emulsion, followed by probe ultrasonication (20 kHz, 750 W) at 50% amplitude for 10 min using 30 s on/30 s off cycles in an ice bath to avoid excessive heating (Vichare & Janjic, 2025).

Sixteen nanoemulsion formulations were prepared using four different surfactant systems: Poloxamer 188 (PF), Quillaja saponin (SF), Cremophor® RH40 (CF), and hybrid Cremophor® RH40/Quillaja saponin (FC). The composition of all formulations is presented in Table 1.

Table 1. Composition of nanoemulsion formulations prepared during formulation screening

Component (% w/w)	PF1	PF2	PF3	SF1	SF2	SF3	SF4	SF5	CF4	CF5	CF6	CF7	FC1	FC2	FC3	FC4
Oil phase components																
DL-α-Tocopheryl acetate	0.2	0.2	0.2	0.2	0.2	0.2	0.2	0.2	0.2	0.2	0.2	0.2	0.2	0.2	0.2	0.2
Amaranth oil	2	2	2	2	2	2	2	2	2	2	2	2	2	2	2	2
Caprylic/capric triglyceride	3.3	3.3	3.3	3.3	3.3	3.3	3.3	3.3	3.3	3.3	3.3	3.3	3.3	3.3	3.3	3.3
Sensiva® PA 30	2	2	2	2	2	2	2	2	2	2	2	2	2	2	2	2
Labrasol®	2.5	2.5	2.5	2.5	2.5	2.5	2.5	2.5	2.5	2.5	2.5	2.5	2.5	2.5	2.5	2.5
Transcutol® HP	2.5	2.5	2.5	2.5	2.5	2.5	2.5	2.5	2.5	2.5	2.5	2.5	2.5	2.5	2.5	2.5
Aqueous phase components																
Poloxamer 188	5	7.5	10	—	—	—	—	—	—	—	—	—	—	—	—	—
Quillaja saponin	—	—	—	0.5	1	2	0.3	0.3	—	—	—	—	0.5	1	0.5	1
Cremophor® RH40	—	—	—	—	—	—	—	—	10	10	7.5	5	10	10	10	10
PEG 400	—	—	—	—	—	—	—	4	—	4	—	—	—	—	4	4
Kemigran® 40	1	1	1	1	1	1	1	1	1	1	1	1	1	1	1	1
Distilled water	81.5	79	76.5	86	85.5	84.5	86.2	82.2	76.5	72.5	79	81.5	76	75.5	72	71.5

PF, poloxamer 188-based formulations; SF, Quillaja saponin-based formulations; CF, Cremophor® RH40-based formulations; FC, hybrid formulations containing Cremophor® RH40 and Quillaja saponin

Screening of nanoemulsions

Freshly prepared nanoemulsions were screened based on droplet size, polydispersity index (PDI), visual appearance, and performance under short-term physical stress conditions. Only formulations that maintained acceptable physicochemical characteristics after centrifugation and thermal stress tests were selected for nanoemulgel preparation. Visual evaluation included the assessment of phase separation, creaming, sedimentation, and coalescence. Droplet size and PDI were determined by dynamic light scattering using a Zetasizer Nano ZS (Malvern Instruments Ltd., Worcestershire, UK). Before analysis, samples were diluted 1:100 (v/v) with ultrapure water and measured at 25 ± 0.5 °C in triplicate.

Short-term physical stress tests

Centrifugation test

Aliquots of each nanoemulsion were transferred into 1.5 mL polypropylene microcentrifuge tubes and centrifuged at 3500 rpm (approximately 1192 × g) for

30 min at room temperature using a Heraeus Biofuge Primo R centrifuge equipped with a 75007593 rotor. The formulations were visually evaluated for phase separation, creaming, sedimentation, and coalescence, followed by droplet size and PDI measurements.

Thermal stress test

Nanoemulsions that remained stable after centrifugation were subjected to thermal stress testing (Mohd Narawi et al., 2020). For each formulation, separately prepared batches were assigned to the 40, 60, and 80 °C conditions, with one batch per temperature. Each batch was incubated at its assigned temperature for 30 min, cooled to room temperature, visually inspected for physical instability, and subsequently analyzed for droplet size and PDI.

Preparation of nanoemulgels

Nanoemulgels were prepared by mixing the selected nisin-free nanoemulsions with xanthan gum gel bases (1.0%, 1.5%, or 2.0%, w/w) at a 1:1 (w/w) ratio (Mulia, Ramadhan, & Krisanti, 2018). Accordingly, the final xanthan gum concentrations in the nanoemulgels were 0.5%, 0.75%, and 1.0% (w/w), respectively. Formulation codes refer to the xanthan gum concentration of the hydrogel base. Nisin (0.1%, w/w) was incorporated into the xanthan gum gel base before the gel base was mixed with the preformed, nisin-free nanoemulsion at a 1:1 (w/w) ratio. The resulting nanoemulgels therefore contained 0.05% (w/w) nominal nisin. The formulations were allowed to stand at room temperature before characterization to remove entrapped air bubbles.

Screening of nanoemulgels

Prepared nanoemulgels were screened based on their visual appearance, droplet size, PDI, zeta potential, and performance under short-term physical stress conditions. Visual assessment included color, homogeneity, consistency, phase separation, creaming, sedimentation, and the presence of visible aggregates. Only formulations showing homogeneous appearance and acceptable physicochemical characteristics under the applied short-term physical stress conditions were selected for further characterization. Droplet size and PDI were determined using the same procedure described for nanoemulsions. Zeta potential was measured using a Zetasizer Nano ZS (Malvern Instruments Ltd., Worcestershire, UK) after 1:100 (v/v) dilution with ultrapure water at 25 ± 0.5 °C. Three aliquots from the same formulation batch were measured separately (n = 3 technical measurements).

Short-term physical stress testing

Nanoemulgels were subjected to the same centrifugation and thermal stress procedures used for the nanoemulsions. Following each test, formulations were visually inspected, and droplet size, PDI, and zeta potential were determined.

Characterization of the selected nanoemulgel

Following the screening studies, the nanoemulgel formulation selected on the basis of its physicochemical characteristics and short-term physical stress results was evaluated for pH, electrical conductivity, and rheological behavior.

pH and electrical conductivity

The pH and electrical conductivity of the selected nanoemulgel were measured at room temperature using calibrated pH and conductivity meters (Hanna Instruments, USA), respectively. Measurements were performed in triplicate, and the results were expressed as mean ± standard deviation.

Rheological evaluation

The rheological behavior of the selected nanoemulgel was evaluated using a Brookfield cone-and-plate viscometer equipped with a CP40 spindle (Brookfield Engineering Laboratories, Middleboro, MA, USA) at 25 ± 0.5 °C over a rotational speed range of 10–100 rpm (Aldeeb et al., 2024). Apparent viscosity and shear stress were recorded at the corresponding shear rates. Flow behavior was analyzed using the Power Law model ($\tau = K\gamma^n$), where K is the consis-

tency index and n is the flow behavior index. The coefficient of determination (R^2) was used to assess the goodness of fit.

Antimicrobial activity

Agar well diffusion method

The antibacterial activity of the active and placebo nanoemulgels against *S. aureus* ATCC 29213 and *S. epidermidis* ATCC 12228 was evaluated using the agar well diffusion method (Humphries, Bobenchik, Hindler, & Schuetz, 2021; Valgas, Souza, Smânia, & Smânia Jr, 2007). Bacterial suspensions adjusted to a 0.5 McFarland standard were inoculated onto Mueller–Hinton agar plates, and 50 µL of each formulation was applied to 7-mm wells. Azithromycin (15 µg) discs served as positive controls. After incubation at 37 °C for 24 h, inhibition zones were measured. The agar well diffusion assay was performed in duplicate (n = 2).

Determination of minimum inhibitory concentration

The minimum inhibitory concentrations (MICs) of the active and placebo nanoemulgels were determined by the broth microdilution method according to CLSI guidelines (Humphries et al., 2021). Two-fold serial dilutions of the formulations were prepared in Mueller–Hinton broth and inoculated with bacterial suspensions adjusted to a 0.5 McFarland standard. Ciprofloxacin was used as the positive control and was evaluated using the same broth microdilution procedure with two-fold serial dilutions. After incubation at 37 °C for 24 h, the MIC was defined as the lowest concentration of the tested formulation or ciprofloxacin that completely inhibited visible bacterial growth.

Data presentation

For physicochemical characterization, three aliquots were measured from the batch assigned to each formulation and experimental condition. Results are presented as mean ± standard deviation (SD) of these three technical measurements. Separate batches were prepared for the different thermal stress conditions; however, each formulation–temperature combination was represented by one batch. Therefore, comparisons between formulations and temperature conditions were interpreted descriptively, without treating technical measurements or batches assigned to different conditions as independent replicates of the same condition. Agar well diffusion results were obtained in duplicate (n = 2) and are reported separately from the triplicate technical measurements used for physicochemical characterization.

RESULTS AND DISCUSSION

Screening of nanoemulsion formulations

A systematic screening strategy was employed to develop a physically stable nanoemulsion for topical nisin delivery. Sixteen formulations were prepared using four surfactant systems: Poloxamer 188 (PF), Quillaja saponin (SF), Cremophor® RH40 (CF), and hybrid Cremophor® RH40/Quillaja saponin (FC) (Table 1). Formulations were evaluated based on visual appearance, droplet size, PDI, and performance under short-term physical stress conditions.

All PF formulations exhibited rapid phase separation despite increasing the Poloxamer 188 concentration from 5% to 10% (w/w), indicating insufficient stabilization of the complex lipid phase, consistent with previous reports (Callender & Wettig, 2021; Magrode, Poomanee, Kiattisin, & Ampasavate, 2024). Similarly, although Quillaja saponin improved emulsification compared with the PF series, none of the SF formulations fulfilled the predefined selection criteria, suggesting that saponin alone was insufficient to stabilize the formulation (Banerjee, Binder, Salama, & Trant, 2021; Schreiner et al., 2020).

In contrast, Cremophor® RH40 markedly improved nanoemulsion stability and physical appearance because of its efficient steric stabilization (Zeng, Liu, Pan, & Liu, 2019). CF5, which contained PEG 400, showed a smaller measured droplet size than the corresponding formulation without PEG 400 (CF4: 131.1 ± 3.2 vs 156.0 ± 2.6 nm). This observed difference, together with its appearance and short-term

physical stress testing results, supported the selection of CF5 for further evaluation (Alnemer, Hussain, & Altamimi, 2025; Astuti, Suliatin, & Wahyuningrum, 2019).

Hybrid formulations combining Cremophor® RH40 and Quillaja saponin were subsequently prepared to further evaluate the surfactant system. Among all formulations, CF5 and FC3 exhibited the most favorable physicochemical characteristics and performance under short-term physical stress conditions and were therefore selected for nanoemulgel preparation using xanthan gum concentrations of 1.0%, 1.5%, and 2.0% (w/w). The selected formulations were subsequently characterized in detail to select a nanoemulgel formulation for further evaluation.

Droplet size and polydispersity index of nanoemulsions

The droplet size and PDI results are presented in Table 2. Among the Cremophor® RH40-based formulations, CF5 exhibited a smaller measured droplet size than CF4 (131.1 ± 3.2 vs 156.0 ± 2.6 nm). Similarly, FC3 showed the most favorable droplet size and PDI among the hybrid formulations. Both CF5 and FC3 exhibited PDI values below 0.15, indicating relatively narrow droplet size distributions (Battisti et al., 2025; Ijaz et al., 2025).

Table 2. Mean droplet size and polydispersity index (PDI) values of the selected nanoemulsion formulations determined immediately after preparation (mean ± SD of three technical measurements from the batch measured for each formulation)

Formulation group	Code	Droplet size (nm)	PDI
Cremophor® RH40	CF4	156.0 ± 2.6	0.091 ± 0.046
	CF5	131.1 ± 3.2	0.110 ± 0.019
Hybrid (Cremophor® RH40 + Quillaja saponin)	FC1	138.3 ± 3.0	0.098 ± 0.012
	FC2	119.2 ± 1.0	0.146 ± 0.019
	FC3	115.3 ± 1.8	0.091 ± 0.019

The measured properties of CF5 may reflect the combined contributions of Cremophor® RH40 and PEG 400, both of which can influence interfacial characteristics and droplet formation (Alnemer et al., 2025; Hashemnejad, Badruddoza, Zarket, Ricardo Castaneda, & Doyle, 2019). Likewise, the combination of Cremophor® RH40 and Quillaja saponin in FC3 may have provided complementary steric and electrosteric stabilization, contributing to its favorable physicochemical characteristics. Based on droplet size, PDI, and visual appearance, CF5 and FC3 were selected for nanoemulgel preparation and further characterization.

Short-term physical stress evaluation of nanoemulsions

Centrifugation test

The selected nanoemulsions were subjected to centrifugation to assess their response to centrifugal stress. Following centrifugation, CF4, CF5, FC1, FC2, and FC3 remained visually homogeneous without phase separation, creaming, sedimentation, or coalescence. Only minor changes in droplet size and PDI were observed (Table 3.), consistent with limited physical changes under the applied centrifugal stress. Similar observations have been reported for kinetically stable nanoemulsions resistant to centrifugal stress (de Oliveira Felipe et al., 2024; Feng et al., 2022).

Thermal stress test

Nanoemulsions that passed the centrifugation test were subsequently exposed to 40, 60, and 80 °C. No visible signs of phase separation were observed after thermal treatment. Droplet size and PDI changed relatively little at 40 and 60 °C, whereas several formulations showed marked increases at 80 °C (Table 3). Thus, the measurements indicate reduced physical stability under the highest temperature condition.

Table 3. Effect of centrifugation and thermal stress on droplet size and PDI of the selected nanoemulsion formulations (mean ± SD of three technical measurements from the batch used for each formulation–condition combination)

Formulation	Condition	Droplet size (nm)	PDI
CF4	Centrifugation	159.13 ± 1.45	0.048 ± 0.041
	40 °C	158.13 ± 1.90	0.094 ± 0.015
	60 °C	166.33 ± 2.41	0.027 ± 0.017
	80 °C	269.37 ± 7.05	0.337 ± 0.008
CF5	Centrifugation	133.30 ± 2.43	0.070 ± 0.030
	40 °C	133.57 ± 0.55	0.078 ± 0.032
	60 °C	140.20 ± 2.33	0.048 ± 0.040
	80 °C	205.83 ± 2.00	0.241 ± 0.011
FC1	Centrifugation	136.10 ± 0.95	0.086 ± 0.025
	40 °C	142.40 ± 1.95	0.100 ± 0.034
	60 °C	138.77 ± 0.32	0.116 ± 0.016
	80 °C	354.40 ± 2.36	0.164 ± 0.019
FC2	Centrifugation	120.03 ± 0.76	0.112 ± 0.016
	40 °C	120.20 ± 1.84	0.181 ± 0.009
	60 °C	130.07 ± 0.90	0.197 ± 0.032
	80 °C	746.27 ± 11.59	0.533 ± 0.096
FC3	Centrifugation	118.83 ± 0.98	0.099 ± 0.041
	40 °C	115.13 ± 0.68	0.071 ± 0.037
	60 °C	126.17 ± 1.72	0.051 ± 0.027
	80 °C	270.53 ± 5.94	0.180 ± 0.010

Overall, CF5 and FC3 remained visually homogeneous and showed relatively small changes in droplet size and PDI following centrifugation and exposure to 40 and 60 °C. Both showed larger changes at 80 °C; their overall screening results supported their selection for nanoemulgel preparation.

Development and characterization of nanoemulgels

Based on their favorable physicochemical properties and performance under short-term physical stress conditions, CF5 and FC3 were selected for nanoemulgel development. Each nanoemulsion was incorporated into xanthan gum hydrogels containing 1.0%, 1.5%, and 2.0% (w/w) xanthan gum, yielding six nanoemulgel formulations.

All formulations exhibited homogeneous appearance without visible phase separation, oil droplets, or precipitation (Figure 1). The CF5 formulations appeared opaque white, whereas the FC3 formulations showed a slightly cream-colored appearance. Increasing xanthan gum concentration increased gel consistency, and the 1.5% formulations showed a homogeneous appearance and suitable consistency and handling characteristics (Mustafa, Mohd Amin, Zakaria, Anuar, & Baharuddin, 2025; Tošić et al., 2025).

Hydrolyzed wheat protein (Kemigran® 40) was included for its reported skin-conditioning and film-forming properties (Burnett et al., 2018). Its concentration was kept constant across formulations during the comparison of different surfactant systems and xanthan gum concentrations. As no formulation without Kemigran® 40 was prepared, its individual effects on formulation properties, skin hydration, or barrier function cannot be determined from this study. The wheat origin of this ingredient also mer-

its consideration for its intended use on atopic skin. Sensitization following topical exposure to certain hydrolyzed wheat protein-containing products has been reported, including in a patient with atopic dermatitis (Brockow, Reidenbach, Kugler, & Biedermann, 2022). Published cosmetic safety assessments emphasize the molecular-weight characteristics of the hydrolysate (Burnett et al., 2018); therefore, characterization of the ingredient used and assessment of the finished formulation's skin tolerability would be appropriate in further development.

Droplet size, polydispersity index, and zeta potential of nanoemulgels

The droplet size, PDI, and zeta potential values of the nanoemulgel formulations are presented in Table 4. Following incorporation into the xanthan gum gels, the diluted samples exhibited nanometric droplet sizes under the applied DLS measurement conditions (Mustafa et al., 2025; Tošić et al., 2025).

Table 4. Physicochemical characterization of the nanoemulgel formulations (mean ± SD of three technical measurements from the batch measured for each formulation)

Formulation	Droplet size (nm)	PDI	Zeta potential (mV)
FC3-1% NEJ	126.03 ± 0.60	0.19 ± 0.01	−30.13 ± 0.64
FC3-1.5% NEJ	110.40 ± 0.96	0.17 ± 0.02	−40.40 ± 5.86
FC3-2% NEJ	159.23 ± 3.77	0.16 ± 0.02	−34.00 ± 2.26
CF5-1% NEJ	151.37 ± 1.78	0.18 ± 0.03	−25.90 ± 3.21
CF5-1.5% NEJ	167.57 ± 0.84	0.22 ± 0.01	−34.97 ± 0.32
CF5-2% NEJ	157.43 ± 0.55	0.23 ± 0.02	−37.03 ± 4.57

Xanthan gum concentration influenced the physicochemical characteristics of both nanoemulgel systems. In the FC3 formulations, droplet size decreased at 1.5% xanthan gum but increased at 2.0%, whereas the CF5 formulations exhibited only minor variations across the tested polymer concentrations. All formulations showed low PDI values (0.16–0.23), indicating relatively narrow droplet size distributions under the diluted DLS measurement conditions. However, because the nanoemulgels were diluted 1:100 (v/v) before DLS analysis, the measured hydrodynamic droplet size and PDI values reflect the dispersed droplets under diluted measurement conditions and may not fully represent droplet organization or interactions within the undiluted gel matrix. Therefore, these results should not be interpreted as a direct characterization of the intact nanoemulgel microstructure. Increasing xanthan gum concentration beyond 1.5% did not result in a consistent reduction in the measured droplet size or PDI under the applied DLS conditions (Mustafa et al., 2025).

All nanoemulgels exhibited negative zeta potential values ranging from −25.9 to −40.4 mV. The more negative zeta potential of the FC3 formulations was likely related to the presence of Quillaja saponin, whereas the negative surface charge of the CF5 formulations was mainly associated with xanthan gum, with Cremophor® RH40 providing additional steric stabilization (Tošić et al., 2025; Wang, Virgilio, Wood-Adams, & Heuzey, 2017). Based on their overall physicochemical characteristics and short-term physical stress testing, the 1.0% and 1.5% xanthan gum nanoemulgels were selected for further biological evaluation.

Short-term physical stress evaluation of nanoemulgels

The short-term physical stress testing results are presented in Table 5, and representative photographs of the formulations after centrifugation and thermal stress testing are shown in Figure 1. None of the nanoemulgels exhibited visible phase separation, creaming, or precipitation after centrifugation or exposure to 40 and 60 °C. Only minor changes in droplet size, PDI, and zeta potential were observed under these conditions (Mustafa et al., 2025; Tošić et al., 2025).

Table 5. Physicochemical characteristics of nanoemulgels after short-term physical stress tests (mean ± SD of three technical measurements from the batch used for each formulation–condition combination)

Formulation	Condition	Droplet size (nm)	PDI	Zeta potential (mV)
FC3-1%	Centrifugation	124.20 ± 1.85	0.14 ± 0.02	−27.43 ± 1.70
	40 °C	117.77 ± 0.85	0.16 ± 0.01	−31.77 ± 4.20
	60 °C	124.67 ± 0.75	0.14 ± 0.01	−28.93 ± 7.81
	80 °C	763.30 ± 43.80	0.92 ± 0.13	−16.40 ± 0.20
FC3-1.5%	Centrifugation	135.27 ± 0.38	0.30 ± 0.04	−30.17 ± 2.15
	40 °C	127.07 ± 13.16	0.31 ± 0.09	−31.13 ± 2.82
	60 °C	117.57 ± 1.52	0.19 ± 0.01	−41.90 ± 4.88
	80 °C	499.93 ± 37.01	0.52 ± 0.04	−20.50 ± 1.42
FC3-2%	Centrifugation	155.43 ± 0.91	0.21 ± 0.03	−34.47 ± 1.00
	40 °C	155.90 ± 1.44	0.23 ± 0.03	−37.30 ± 4.22
	60 °C	169.40 ± 4.12	0.24 ± 0.03	−32.23 ± 1.42
	80 °C	444.47 ± 20.68	0.50 ± 0.02	−27.30 ± 1.65
CF5-1%	Centrifugation	144.20 ± 1.08	0.13 ± 0.02	−24.17 ± 0.74
	40 °C	147.10 ± 2.82	0.15 ± 0.05	−23.40 ± 1.56
	60 °C	153.67 ± 3.57	0.16 ± 0.04	−22.27 ± 1.18
	80 °C	232.83 ± 3.23	0.21 ± 0.01	−22.67 ± 3.33
CF5-1.5%	Centrifugation	152.33 ± 1.06	0.15 ± 0.02	−33.70 ± 1.40
	40 °C	157.37 ± 5.40	0.22 ± 0.01	−30.97 ± 4.06
	60 °C	157.60 ± 6.52	0.20 ± 0.03	−32.37 ± 1.60
	80 °C	301.83 ± 4.50	0.36 ± 0.03	−29.90 ± 1.91
CF5-2%	Centrifugation	152.17 ± 1.91	0.21 ± 0.02	−29.40 ± 1.93
	40 °C	154.87 ± 4.22	0.22 ± 0.02	−31.00 ± 2.78
	60 °C	163.63 ± 0.91	0.23 ± 0.03	−29.17 ± 1.53
	80 °C	286.17 ± 9.16	0.40 ± 0.07	−28.97 ± 4.01

Following exposure to 80 °C, droplet size and PDI increased in both CF5-1% and CF5-1.5%. CF5-1% showed a droplet size of 232.83 ± 3.23 nm, a PDI of 0.21 ± 0.01, and a zeta potential of −22.67 ± 3.33 mV; the corresponding values for CF5-1.5% were 301.83 ± 4.50 nm, 0.36 ± 0.03, and −29.90 ± 1.91 mV. Both formulations retained submicron droplet sizes under this thermal stress, with CF5-1% showing lower droplet size and PDI values. CF5-1.5% was selected for further characterization and antimicrobial evaluation based on the combined assessment of its homogeneous appearance, suitable gel consistency, physicochemical characteristics, and performance under centrifugation and moderate thermal stress. Subsequent rheological evaluation showed pseudoplastic flow behavior, supporting its suitability as a topical gel formulation.

Nisin is an antimicrobial peptide whose chemical stability has been shown to depend on pH and temperature (Rollema, Kuipers, Both, de Vos, & Siezen, 1995). Ultrasound-induced oxidation and degradation have also been demonstrated for peptides in aqueous solution, although those findings do not establish that nisin is degraded under the specific processing conditions used here (Sakakura & Takayama, 2009). Accordingly, nisin was added to the aqueous xanthan gum gel base after nanoemulsion preparation as a precautionary measure to avoid its exposure to probe ultrasonication and the heating step. Because nisin stability was not compared before and after these processes, a protective effect of this addition sequence cannot be concluded.

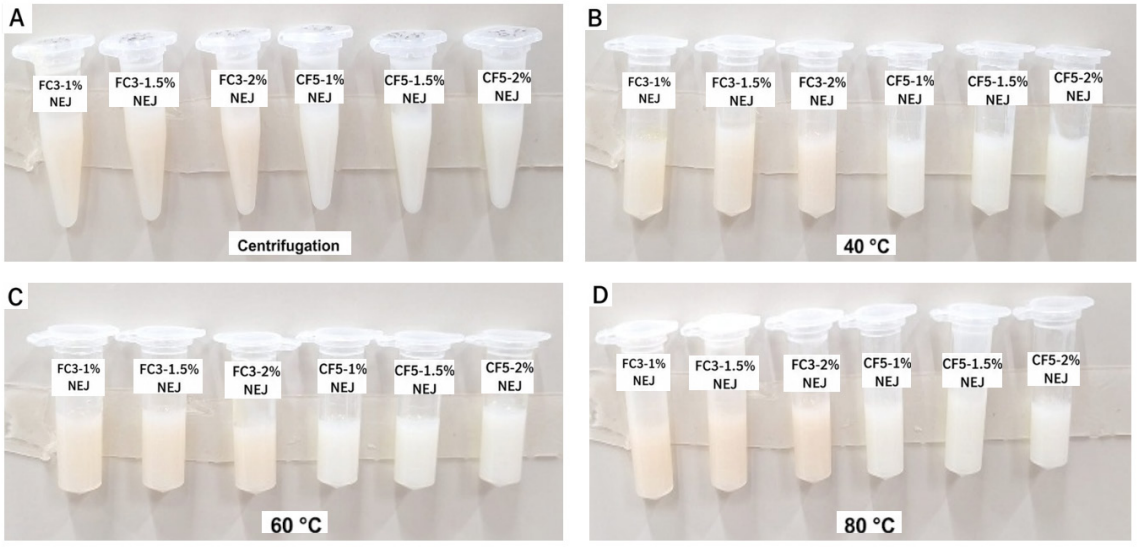

Figure 1. Representative photographs of nanoemulgel formulations following centrifugation and thermal stress testing

pH and electrical conductivity

The selected nanoemulgel prepared using a hydrogel base containing 1.5% xanthan gum exhibited a pH of 5.51 ± 0.01, which is within the physiological skin pH range. This finding is consistent with previous reports on xanthan gum-based nanoemulgels (Donthi et al., 2023; Mustafa et al., 2025).

The electrical conductivity of the formulation was 1757.67 ± 0.58 µS/cm, confirming the presence of a continuous aqueous phase and the oil-in-water (O/W) nature of the nanoemulgel. These findings agree with previous studies reporting O/W nanoemulgels for topical delivery (Donthi et al., 2023; Nastiti et al., 2017).

Rheological evaluation

The rheological behavior of the selected CF5 nanoemulgels containing 1.0% and 1.5% xanthan gum is shown in Figure 2. Both formulations exhibited shear-thinning (pseudoplastic) behavior, with apparent viscosity decreasing as shear rate increased. The apparent viscosity decreased from 117.40 ± 16.19 to 29.63 ± 0.56 cP for the 1.0% xanthan gum formulation and from 222.04 ± 4.16 to 43.85 ± 0.88 cP for the 1.5% formulation over the investigated shear rate range. The higher viscosity of the 1.5% formulation reflects the formation of a stronger gel network, consistent with previous reports on xanthan gum-based hydrogels (Donthi et al., 2023; Tošić et al., 2025).

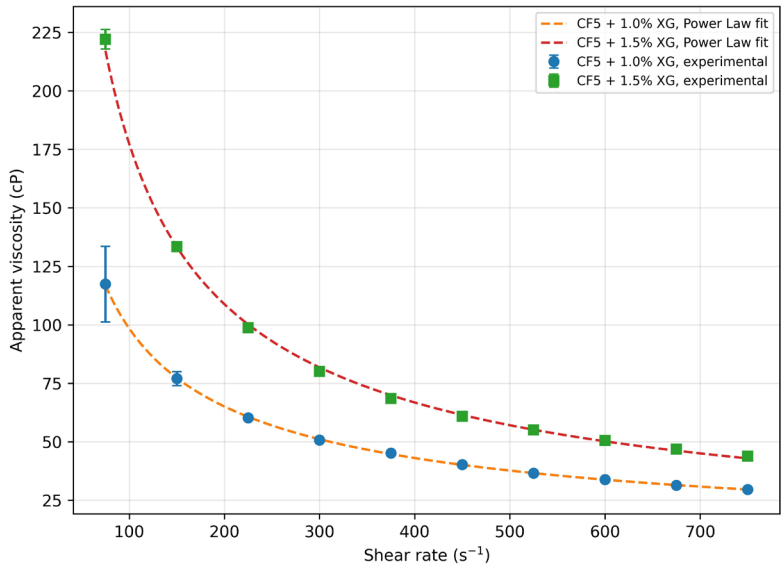

Figure 2. Apparent viscosity as a function of shear rate for CF5 nanoemulgels containing 1.0% and 1.5% xanthan gum with Power Law model fitting. Data are presented as mean ± SD of three technical measurements from the batch measured for each formulation

The experimental data showed excellent agreement with the Power Law model ($R^2 \geq 0.999$). Flow behavior indices (n = 0.404 and 0.296) confirmed pseudoplastic behavior, while the increase in consistency index (K) from 1534.47 to 4542.82 demonstrated enhanced structural strength with increasing xanthan gum concentration. The lower n and higher K values of the 1.5% nanoemulgel indicate more pronounced shear-thinning behavior and greater consistency within the measured shear-rate range (Donthi et al., 2023; Tadros, 2013; Tošić et al., 2025). Skin bioadhesion and residence time were not measured and cannot be inferred from these rheological results alone.

Antimicrobial activity

The antibacterial activity of the nanoemulgels containing nisin in the external xanthan gum gel phase and their corresponding placebo formulations was evaluated against *S. aureus* ATCC 29213 and *S. epidermidis* ATCC 12228. The placebo nanoemulgels showed no detectable antibacterial activity, whereas both nisin-containing nanoemulgels inhibited the growth of the tested bacterial strains. Against *S. aureus*, both nisin-containing formulations produced inhibition zones of 9.5 ± 0.0 mm. Against *S. epidermidis*, the zones were 10.0 ± 0.0 mm for CF5-1% and 9.5 ± 0.0 mm for CF5-1.5% (Table 6). Because these diameters include the 7-mm well, the clear region extended approximately 1.25–1.50 mm beyond the well edge on each side. The small zones indicate detectable inhibition under the assay conditions, but their therapeutic relevance for atopic dermatitis cannot be established from this experiment.

Both nanoemulgels inhibited *S. aureus* at a formulation MIC of 12.5% (v/v). Against *S. epidermidis*, the formulation MICs were 12.5% (v/v) for CF5-1% and 25% (v/v) for CF5-1.5% (Table 6). Based on the nominal nisin loading of 0.05% (w/w), these formulation concentrations correspond to approximately 62.5 and 125 µg/mL nominal nisin input, respectively.

CF5-1% showed a slightly larger inhibition zone and a lower formulation MIC against *S. epidermidis* than CF5-1.5%. These descriptive differences may be influenced by diffusion from the gel matrix, but the

present assays do not establish their mechanism or clinical significance (Cheng et al., 2024). Although the individual contributions of nisin, amaranth oil, and Kemigran® 40 could not be distinguished, the absence of antibacterial activity in the placebo formulations together with the well-established efficacy of nisin against Gram-positive bacteria suggests that nisin was the principal contributor to the observed antibacterial effect (Moretta et al., 2021).

Table 6. Antibacterial activity of the nanoemulgel formulations against *S. aureus* ATCC 29213 and *S. epidermidis* ATCC 12228 determined by agar well diffusion and broth microdilution assays

Formulation	Inhibition zone (mm)		MIC (% v/v)	
	S. aureus	*S. epidermidis*	*S. aureus*	*S. epidermidis*
Placebo nanoemulgel (1% xanthan gum)	–	–	–	–
Placebo nanoemulgel (1.5% xanthan gum)	–	–	–	–
Nisin-containing NEJ (1% xanthan gum)	9.5 ± 0.0	10.0 ± 0.0	12.5	12.5
Nisin-containing NEJ (1.5% xanthan gum)	9.5 ± 0.0	9.5 ± 0.0	12.5	25.0
Azithromycin (15 µg)	23.0 ± 0.0	26.5 ± 0.0	ND	ND
Ciprofloxacin	ND	ND	0.25 µg/mL	0.25 µg/mL

NEJ, nanoemulgel; MIC, minimum inhibitory concentration; ND, not determined.

Inhibition zone diameters include the 7-mm well. Agar well diffusion assays were performed in duplicate (n = 2), and inhibition-zone values are presented as mean ± SD. For the azithromycin positive control, identical values were obtained in both replicate measurements, resulting in an SD of 0.00. Ciprofloxacin was used as the positive control for the broth microdilution assay, and its MIC was determined using two-fold serial dilutions as the lowest concentration completely inhibiting visible bacterial growth. ND: not determined.

In vitro release of nisin from the nanoemulgel matrix was not measured in this study. Nisin was incorporated into the external xanthan gum gel phase, but its location in that phase does not establish its release rate or extent. The agar well diffusion and broth microdilution results provide preliminary evidence of antibacterial activity under the respective assay conditions; they cannot be used to determine nisin release kinetics or predict its availability at the skin surface. Consequently, the influence of xanthan gum concentration on nisin release remains unknown. Quantitative release testing using a suitable validated assay is needed in future work.

CONCLUSION

An amaranth oil nanoemulgel containing hydrolyzed wheat protein and nisin in the external xanthan gum gel phase was successfully developed for potential topical delivery in atopic dermatitis. Based on the combined assessment of physicochemical characteristics, appearance, and gel consistency, the Cremophor® RH40-based nanoemulgel prepared with the hydrogel base containing 1.5% xanthan gum was selected for further evaluation. It exhibited pseudoplastic flow behavior and antibacterial activity against *S. aureus* and *S. epidermidis*. The absence of antibacterial activity in the placebo formulations was consistent with a contribution from nisin to the observed activity. Overall, these findings support further investigation of the selected nanoemulgel as a potential topical formulation containing nisin. Nisin release, skin delivery, and long-term storage stability of the selected nanoemulgel were not evaluated in this study. Quantitative release and skin-delivery studies, further biological evaluation, and storage studies monitoring pH, viscosity, and other relevant quality attributes under controlled temperature and humidity conditions are needed to establish its therapeutic potential and shelf life.

ACKNOWLEDGEMENTS

This study was supported by the Scientific Research Projects Coordination Unit of Istanbul University (Project No: 40805). The authors gratefully acknowledge the Istanbul University Scientific Research Projects Coordination Unit for its financial support.

AUTHOR CONTRIBUTION STATEMENT

Conceptualization (EA); Methodology (EA, CK, MA); Investigation (CK, MA, EA); Formal analysis (EA); Data curation (CK); Writing – Original Draft (EA); Writing – Review & Editing (EA, MA); Supervision (EA); Project administration (EA).

CONFLICT OF INTEREST

The authors declare that they have no conflict of interest.

REFERENCES

Aldeeb, R. A. E., Ibrahim, S. S. A., Khalil, I. A., Ragab, G. M., El-Gazar, A. A., Taha, A. A., . . . Younis, M. K. (2024). Enhancing collagen based nanoemulgel for effective topical delivery of Aceclofenac and Citronellol oil: Formulation, optimization, in-vitro evaluation, and in-vivo osteoarthritis study with a focus on HMGB-1/RAGE/NF-κB pathway, Klotho, and miR-499a. *Drug Delivery and Translational Research, 14*(11), 3250–3268. doi:10.1007/s13346-024-01548-3

Alnemer, O. A., Hussain, A., & Altamimi, M. A. (2025). Solubility prediction and cytotoxicity of lipidic microemulsion: HSPiP modeling and synergism with ciclopirox olamine. *Scientific Reports, 15*, 33663. doi:10.1038/s41598-025-18141-4

Astuti, I. Y., Suliatin, T., & Wahyuningrum, R. (2019). Dissolution enhancement of tetrahydrocurcumin using optimized self-nanoemulsifying drug delivery system. *International Journal of Applied Pharmaceutics, 11*, 97–102. doi:10.22159/ijap.2019.v11s5.T0079

Banerjee, A., Binder, J., Salama, R., & Trant, J. F. (2021). Synthesis, characterization and stress-testing of a robust quillaja saponin stabilized oil-in-water phytocannabinoid nanoemulsion. *Journal of Cannabis Research, 3*(1), 43. doi:10.1186/s42238-021-00094-w

Battisti, A. P., de Matos Fonseca, J., Valencia, G. A., Martins, A. J., Soares, C., Lima, N., . . . Bourbon, A. I. (2025). Antifungal nanoemulsions based on basil essential oil stabilized with saponins extracted from Quillaja lancifolia. *Journal of Molecular Liquids, 443*, 129151. doi:10.1016/j.molliq.2025.129151

Bhattacharya, N., Sato, W. J., Kelly, A., Ganguli-Indra, G., & Indra, A. K. (2019). Epidermal lipids: Key mediators of atopic dermatitis pathogenesis. *Trends in Molecular Medicine, 25*(6), 551–562. doi:10.1016/j.molmed.2019.04.001

Brockow, K., Reidenbach, K., Kugler, C., & Biedermann, T. (2022). Wheat-dependent exercise-induced anaphylaxis caused by percutaneous sensitisation to hydrolysed wheat protein in cosmetics. *Contact Dermatitis, 87*(3), 296–297. doi:10.1111/cod.14144

Burnett, C., Bergfeld, W. F., Belsito, D. V., Hill, R. A., Klaassen, C. D., Liebler, D. C., . . . Snyder, P. W. (2018). Safety assessment of hydrolyzed wheat protein and hydrolyzed wheat gluten as used in cosmetics. *International Journal of Toxicology, 37*(1_suppl), 55S–66S. doi:10.1177/1091581818776013

Byrd, A. L., Deming, C., Cassidy, S. K. B., Harrison, O. J., Ng, W. I., Conlan, S., . . . Kong, H. H. (2017). Staphylococcus aureus and Staphylococcus epidermidis strain diversity underlying pediatric atopic dermatitis. *Science Translational Medicine, 9*(397). doi:10.1126/scitranslmed.aal4651

Callender, S. P., & Wettig, S. D. (2021). Phase behavior of non-ionic surfactant-medium chain triglyceride-water microemulsion systems. *Journal of Surfactants and Detergents, 24*(4), 603–629. doi:10.1002/jsde.12510

Chen, Y., Knight, R., & Gallo, R. L. (2023). Evolving approaches to profiling the microbiome in skin disease. *Frontiers in Immunology, 14*, 1151527. doi:10.3389/fimmu.2023.1151527

Cheng, Z., Kandekar, U., Ma, X., Bhabad, V., Pandit, A., Liu, L., . . . Tao, L. (2024). Optimizing fluconazole-embedded transfersomal gel for enhanced antifungal activity and compatibility studies. *Frontiers in Pharmacology, 15*, 1353791. doi:10.3389/fphar.2024.1353791

de Alcantara Sica de Toledo, L., Rosseto, H. C., Buccini, D. F., & Franco, O. L. (2025). Synergy between antimicrobial peptides and lipid nanoparticles for skin infection control. *ACS Applied Materials & Interfaces, 18*(5), 7740–7754. doi:10.1021/acsami.5c18033

de Oliveira Felipe, L., Bicas, J. L., Changwatchai, T., Abah, E. O., Nakajima, M., & Neves, M. A. (2024). Physical stability of α-terpineol-based nanoemulsions assessed by direct and accelerated tests using photo centrifuge analysis. *LWT, 205*, 116513. doi:10.1016/j.lwt.2024.116513

Dijksteel, G. S., Ulrich, M. M. W., Middelkoop, E., & Boekema, B. (2021). Review: Lessons learned from clinical trials using antimicrobial peptides (AMPs). *Frontiers in Microbiology, 12*, 616979. doi:10.3389/fmicb.2021.616979

Donthi, M. R., Munnangi, S. R., Krishna, K. V., Saha, R. N., Singhvi, G., & Dubey, S. K. (2023). Nanoemulgel: A novel nano carrier as a tool for topical drug delivery. *Pharmaceutics, 15*(1), 164. doi:10.3390/pharmaceutics15010164

Draper, L. A., Cotter, P. D., Hill, C., & Ross, R. P. (2015). Lantibiotic resistance. *Microbiology and Molecular Biology Reviews, 79*(2), 171–191. doi:10.1128/MMBR.00051-14

Eichenfield, L. F., Stripling, S., Fung, S., Cha, A., O'Brien, A., & Schachner, L. A. (2022). Recent developments and advances in atopic dermatitis: A focus on epidemiology, pathophysiology, and treatment in the pediatric setting. *Paediatric Drugs, 24*(4), 293–305. doi:10.1007/s40272-022-00499-x

Feng, X., Feng, K., Zheng, Q., Tan, W., Zhong, W., Liao, C., . . . Hu, W. (2022). Preparation and characterization of geraniol nanoemulsions and its antibacterial activity. *Frontiers in Microbiology, 13*, 1080300. doi:10.3389/fmicb.2022.1080300

George, S. M., Karanovic, S., Harrison, D. A., Rani, A., Birnie, A. J., Bath-Hextall, F. J., . . . Williams, H. C. (2019). Interventions to reduce Staphylococcus aureus in the management of eczema. *Cochrane Database of Systematic Reviews, 2019*(10), CD003871. doi:10.1002/14651858.CD003871.pub3

Goleva, E., Berdyshev, E., & Leung, D. Y. M. (2019). Epithelial barrier repair and prevention of allergy. *Journal of Clinical Investigation, 129*(4), 1463–1474. doi:10.1172/JCI124608

Gonzalez, T., Stevens, M. L., Baatyrbek Kyzy, A., Alarcon, R., He, H., Kroner, J. W., . . . Herr, A. B. (2021). Biofilm propensity of Staphylococcus aureus skin isolates is associated with increased atopic dermatitis severity and barrier dysfunction in the MPAACH pediatric cohort. *Allergy, 76*(1), 302–313. doi:10.1111/all.14489

Hashemnejad, S. M., Badruddoza, A. Z. M., Zarket, B., Ricardo Castaneda, C., & Doyle, P. S. (2019). Thermoresponsive nanoemulsion-based gel synthesized through a low-energy process. *Nature Communications, 10*, 2749. doi:10.1038/s41467-019-10749-1

Hatano, Y., & Elias, P. M. (2023). "Outside-to-inside," "inside-to-outside," and "intrinsic" endogenous pathogenic mechanisms in atopic dermatitis: Keratinocytes as the key functional cells involved in both permeability barrier dysfunction and immunological alterations. *Frontiers in Immunology, 14*, 1239251. doi:10.3389/fimmu.2023.1239251

Humphries, R., Bobenchik, A. M., Hindler, J. A., & Schuetz, A. N. (2021). Overview of changes to the Clinical and Laboratory Standards Institute performance standards for antimicrobial susceptibility testing, M100. *Journal of Clinical Microbiology, 59*(12), e00213-21. doi:10.1128/JCM.00213-21

Ijaz, F., Nasir, B., Rashid, S. A., Naseem, F., Jalil, A., Riaz, A., . . . Azad, A. K. (2025). Colistin adorned topical nanoemulsion gel formulation for enhanced anti-microbial activity. *Scientific Reports, 15*, 34064. doi:10.1038/s41598-025-14440-y

Jacob, S., & Nair, A. B. (2026). Nanoemulgels as advanced topical drug delivery systems: Mechanistic insights and therapeutic applications in skin disorders, infections, wound healing, and cancer. *Pharmaceuticals, 19*(2), 247. doi:10.3390/ph19020247

Kim, J., Kim, B. E., Ahn, K., & Leung, D. Y. M. (2019). Interactions between atopic dermatitis and Staphylococcus aureus infection: Clinical implications. *Allergy, Asthma & Immunology Research, 11*(5), 593–603. doi:10.4168/aair.2019.11.5.593

Kumar, M., Bishnoi, R. S., Shukla, A. K., & Jain, C. P. (2019). Techniques for formulation of nanoemulsion drug delivery system: A review. *Preventive Nutrition and Food Science, 24*(3), 225–234. doi:10.3746/pnf.2019.24.3.225

Kwatra, S. G., Gruben, D., Fung, S., & DiBonaventura, M. (2021). Psychosocial comorbidities and health status among adults with moderate-to-severe atopic dermatitis: A 2017 US National Health and Wellness Survey analysis. *Advances in Therapy, 38*(3), 1627–1637. doi:10.1007/s12325-021-01630-z

Lal, D. K., Kumar, B., Saeedan, A. S., & Ansari, M. N. (2023). An overview of nanoemulgels for bioavailability enhancement in inflammatory conditions via topical delivery. *Pharmaceutics, 15*(4), 1187. doi:10.3390/pharmaceutics15041187

Magrode, N., Poomanee, W., Kiattisin, K., & Ampasavate, C. (2024). Microemulsions and nanoemulsions for topical delivery of tripeptide-3: From design of experiment to anti-sebum efficacy on facial skin. *Pharmaceutics, 16*(4), 554. doi:10.3390/pharmaceutics16040554

Malik, M. R., Nawaz, A., & Noor, W. (2024). The nanoemulsion technique, one of the most promising strategies for enhancing drug permeation through transdermal route. In J. C. Mejuto & M. Poša (Eds.), *Design and applications of self-assembly aggregates: From micelles to nanoemulsions*. London, UK: IntechOpen. doi:10.5772/intechopen.1005267

Martirosyan, D., Hutcheson, J., Sajitharan, D., Williams, S., & Mohan, C. (2021). The effect of amaranth oil on proteinuria in lupus prone mice. *Functional Food Science, 1*(10), 39–49. doi:10.31989/ffs.v1i10.848

Mohd Narawi, M., Chiu, H. I., Yong, Y. K., Mohamad Zain, N. N., Ramachandran, M. R., Tham, C. L., . . . Lim, V. (2020). Biocompatible nutmeg oil-loaded nanoemulsion as phyto-repellent. *Frontiers in Pharmacology, 11*, 214. doi:10.3389/fphar.2020.00214

Moretta, A., Scieuzo, C., Petrone, A. M., Salvia, R., Manniello, M. D., Franco, A., . . . Falabella, P. (2021). Antimicrobial peptides: A new hope in biomedical and pharmaceutical fields. *Frontiers in Cellular and Infection Microbiology, 11*, 668632. doi:10.3389/fcimb.2021.668632

Mulia, K., Ramadhan, R. M. A., & Krisanti, E. A. (2018). Formulation and characterization of nanoemulgel mangosteen extract in virgin coconut oil for topical formulation. *MATEC Web of Conferences, 156*, 01013. doi:10.1051/matecconf/201815601013

Mustafa, H. M., Mohd Amin, N. A., Zakaria, R., Anuar, M. S., & Baharuddin, A. S. (2025). Effect of gelatin/xanthan gum ratios on jackfruit leaf extract nanoemulsion gel stability and properties. *BioResources, 20*(1), 2056–2070. doi:10.15376/biores.20.1.2056-2070

Nasirpour-Tabrizi, P., Azadmard-Damirchi, S., Hesari, J., & Piravi-Vanak, Z. (2020). Amaranth seed oil composition. In V. Y. Waisundara (Ed.), *Nutritional value of amaranth*. London, UK: IntechOpen. doi:10.5772/intechopen.91381

Nastiti, C. M., Ponto, T., Abd, E., Grice, J. E., Benson, H. A., & Roberts, M. S. (2017). Topical nano and microemulsions for skin delivery. *Pharmaceutics, 9*(4), 37. doi:10.3390/pharmaceutics9040037

Preet, S., Kaur, J., & Raza, K. (2021). Nisin loaded carbopol gel against Pseudomonas aeruginosa infected third-degree burns: A therapeutic intervention. *Wound Repair and Regeneration, 29*(5), 711–724. doi:10.1111/wrr.12909

Reczyńska-Kolman, K., Hartman, K., Kwiecień, K., Brzychczy-Włoch, M., & Pamuła, E. (2021). Composites based on gellan gum, alginate and nisin-enriched lipid nanoparticles for the treatment of infected wounds. *International Journal of Molecular Sciences, 23*(1), 321. doi:10.3390/ijms23010321

Rollema, H. S., Kuipers, O. P., Both, P., de Vos, W. M., & Siezen, R. J. (1995). Improvement of solubility and stability of the antimicrobial peptide nisin by protein engineering. *Applied and Environmental Microbiology, 61*(8), 2873–2878. doi:10.1128/AEM.61.8.2873-2878.1995

Sakakura, M., & Takayama, M. (2009). Sonolytic hydrolysis of peptides in aqueous solution upon addition of catechol. *Ultrasonics Sonochemistry, 16*(3), 367–371. doi:10.1016/j.ultsonch.2008.09.006

Schreiner, T. B., Santamaria-Echart, A., Ribeiro, A., Peres, A. M., Dias, M. M., Pinho, S. P., & Barreiro, M. F. (2020). Formulation and optimization of nanoemulsions using the natural surfactant saponin from quillaja bark. *Molecules, 25*(7), 1538. doi:10.3390/molecules25071538

Sghier, K., Mur, M., Veiga, F., Paiva-Santos, A. C., & Pires, P. C. (2024). Novel therapeutic hybrid systems using hydrogels and nanotechnology: A focus on nanoemulgels for the treatment of skin diseases. *Gels, 10*(1), 45. doi:10.3390/gels10010045

Tadros, T. F. (2013). Emulsion formation, stability, and rheology. In T. F. Tadros (Ed.), *Emulsion formation and stability* (pp. 1–75). Weinheim, Germany: Wiley-VCH. doi:10.1002/9783527647941.ch1

Tavares, T. D., Ribeiro, A. R. M., Silva, C., Antunes, J. C., & Felgueiras, H. P. (2024). Combinatory effect of nisin antimicrobial peptide with bioactive molecules: A review. *Journal of Drug Delivery Science and Technology, 91*, 105246. doi:10.1016/j.jddst.2023.105246

Tier, H. L., Balogh, E. A., Bashyam, A. M., Fleischer, A. B., Jr., Spergel, J. M., Masicampo, E. J., . . . Feldman, S. R. (2021). Tolerability of and adherence to topical treatments in atopic dermatitis: A narrative review. *Dermatology and Therapy, 11*(2), 415–431. doi:10.1007/s13555-021-00500-4

Tošić, A., Randjelović, D., Ivković, B., Gledović, A., Stanković, T., Đoković, J., . . . Pantelić, I. (2025). Interfacial molecular interactions as determinants of nanostructural preservation in ibuprofen-loaded nanoemulsions and nanoemulsion gels. *Pharmaceutics, 17*(12), 1532. doi:10.3390/pharmaceutics17121532

Totté, J., van der Feltz, W., Hennekam, M., van Belkum, A., van Zuuren, E., & Pasmans, S. (2016). Prevalence and odds of Staphylococcus aureus carriage in atopic dermatitis: A systematic review and meta-analysis. *British Journal of Dermatology, 175*(4), 687–695. doi:10.1111/bjd.14566

Valenta, C., Bernkop-Schnürch, A., & Rigler, H. P. (1996). The antistaphylococcal effect of nisin in a suitable vehicle: A potential therapy for atopic dermatitis in man. *Journal of Pharmacy and Pharmacology, 48*(9), 988–991. doi:10.1111/j.2042-7158.1996.tb06019.x

Valgas, C., Souza, S. M. d., Smânia, E. F., & Smânia Jr., A. (2007). Screening methods to determine antibacterial activity of natural products. *Brazilian Journal of Microbiology, 38*(2), 369–380. doi:10.1590/S1517-83822007000200034

Vichare, R., & Janjic, J. (2025). Perfluorocarbon nanoemulsions in drug delivery: Design, development, and manufacturing. *Theranostics, 15*(7), 3013–3034. doi:10.7150/thno.103820

Wang, C.-S., Virgilio, N., Wood-Adams, P., & Heuzey, M.-C. (2017). A mechanism for the synergistic gelation properties of gelatin B and xanthan gum aqueous mixtures. *Carbohydrate Polymers, 175*, 484–492. doi:10.1016/j.carbpol.2017.08.015

Wiedemann, I., Breukink, E., van Kraaij, C., Kuipers, O. P., Bierbaum, G., de Kruijff, B., & Sahl, H.-G. (2001). Specific binding of nisin to the peptidoglycan precursor lipid II combines pore formation and inhibition of cell wall biosynthesis for potent antibiotic activity. *Journal of Biological Chemistry, 276*(3), 1772–1779. doi:10.1074/jbc.M006770200

Wollenberg, A., Christen-Zäch, S., Taieb, A., Paul, C., Thyssen, J. P., de Bruin-Weller, M., . . . Ring, J. (2020). ETFAD/EADV Eczema task force 2020 position paper on diagnosis and treatment of atopic dermatitis in adults and children. *Journal of the European Academy of Dermatology and Venereology, 34*(12), 2717–2744. doi:10.1111/jdv.16892

Zeng, L., Liu, Y., Pan, J., & Liu, X. (2019). Formulation and evaluation of norcanthridin nanoemulsions against the Plutella xylostella (Lepidoptera: Plutellidae). *BMC Biotechnology, 19*(1), 16. doi:10.1186/s12896-019-0508-8